Antibody Therapeutics, 2022, Vol. 5, No. 2 ***138–149***
https://doi.org/10.1093/abt/tbac012
Advance Access Publication on 9 June 2022

Original research article

Development of a T cell-redirecting bispecific antibody targeting B-cell maturation antigen for the suppression of multiple myeloma cell growth

Jianxin Huo[1,†], Yuhan Huang[1,†], Ziying Zheng[2], Xin Ni Tay[2], Farouq Bin Mahfut[2], Wei Zhang[2], Kong-Peng Lam[1,3,*], Yuansheng Yang[2,*] and Shengli Xu[1,4,*]

[1]Singapore Immunology Network, Agency for Science, Technology and Research, 8A Biomedical Grove, Immunos Building, Singapore 138648, Singapore , [2]Bioprocessing Technology Institute, Agency for Science, Technology and Research, 20 Biopolis Way, Centros Building, Singapore 138668, Singapore , [3]Department of Microbiology and Immunology, Yong Loo Lin School of Medicine, 5 Science Drive 2, MD4, National University of Singapore, Singapore 117545, Singapore, and [4]Department of Physiology, Yong Loo Lin School of Medicine, 2 Medical Drive, MD9, National University of Singapore, Singapore 117593, Singapore

Received: April 13, 2022; Revised: May 13, 2022; Accepted: May 18, 2022

ABSTRACT

Background: Multiple myeloma (MM) is the second most common hematological malignancy. It has emerged as one of the next possible hematological diseases amenable to immunotherapy. B-cell maturation antigen (BCMA), a member of the tumor necrosis factor receptor superfamily, is highly expressed in MM cells and is one target with the most potential for developing MM-targeting immunotherapy. Other than the FDA-approved BCMA-targeting CAR T-cell therapy, such as Abecma and CARVYKTI, T cell-engaging multi-specific antibody is another promising therapeutic modality for BCMA-targeting MM treatment. We develop a T-cell redirecting BCMA-targeting bispecific antibody (bsAb) and evaluate its anti-MM activity.

Methods: We first generated several clones of mouse anti-human BCMA monoclonal antibodies using DNA immunization. One of the anti-BCMA antibodies was then used to design and produce a T cell-redirecting BCMA × CD3 bsAb in CHO cells. Finally, we examined the effect of the bsAb on MM cell growth both *in vitro* and *in vivo*.

Results: The BCMA × CD3 bsAb was designed in a FabscFv format and produced in CHO cells with good yield and purity. Moreover, the bsAb can trigger robust T cell proliferation and activation and induce efficient T cell-mediated MM cell killing *in vitro*. Using a MM xenograft mouse model, we demonstrate that the bsAb can effectively suppress MM cell growth *in vivo*.

Conclusions: Our results suggest that the BCMA × CD3 bsAb in the FabscFv format can efficiently inhibit MM cell growth and have promising potential to be developed into a therapeutic antibody drug for the treatment of MM.

Statement of Significance: We have produced a T cell-redirecting BCMA-targeting bsAb that can robustly stimulate T cell proliferation and activation and effectively kill MM cells both *in vitro* and *in vivo*. The BCMA bsAb has good potential to be developed into a therapeutic drug for MM treatment.

KEYWORDS: bispecific antibody; BCMA; multiple myeloma; therapeutic

*To whom correspondence should be addressed. Shengli Xu. Email: xu_shengli@immunol.a-star.edu.sg; Yuansheng Yang. Email: yang_yuansheng@bti.a-star.edu.sg; Kong-Peng Lam. Email: lam_kong_peng@immunol.a-star.edu.sg

†These authors contributed equally to this work.

INTRODUCTION

Multiple myeloma (MM) is an aggressive malignant B-cell neoplasm characterized by the uncontrolled growth and detrimental accumulation of cancerous plasma cells in the bone marrow (BM) [1, 2]. The past two decades have seen considerable advancement in the treatment of MM, such as immunomodulatory drug lenalidomide, proteasome inhibitor bortezomib, and monoclonal antibodies Elotuzumab and Daratumumab that target signalling lymphocytic activation molecule F7 and CD38, respectively [3–6]. However, MM remains largely incurable, as most MM patients become resistant to the prior treatment and eventually succumb to the disease [7, 8]. Hence, it is imperative to develop new effective therapies to treat relapsed/refractory (RR) MM.

The growth and survival of MM cells are dependent on the BM microenvironment that provides a niche and protects the MM cells from spontaneous and drug-induced apoptosis. The communication between MM and BM stromal cells is mainly mediated by soluble factors and adhesion molecules [9]. B-cell activating factor (BAFF) and a proliferation-inducing ligand (APRIL) are two critical factors essential for MM growth and survival [10]. Both BAFF and APRIL belong to the tumor necrosis factor (TNF) ligand superfamily and bind two receptors called B cell maturation antigen (BCMA) and transmembrane activator and CAML interactor (TACI) [11], which are members of TNF receptor superfamily, to support plasma cell survival [10, 12, 13].

In line with the crucial roles of BAFF and APRIL in MM, BCMA and TACI were found to be highly expressed on MM cells and mediate the signal transduction triggered by BAFF and APRIL to support MM growth and survival [14, 15]. The essential roles and the specific expression pattern of BCMA and TACI in MM make them promising targets for developing novel therapeutics for RRMM [16]. Recently, several BCMA-targeting therapeutic modalities, including antibody–drug conjugates (ADCs) and chimeric antigen receptor (CAR)-T cell therapy [14], have been approved by the FDA to treat RRMM. T cell-redirecting BCMA-targeting bispecific antibodies (bsAbs) are also promising therapeutic modalities being evaluated preclinically and clinically [17]. However, some challenges exist in developing BCAM-targeting bsAb, such as variable yield and functionality, poor stability and solubility of the antibody produced in different bsAb formats. Therefore, there is a need to produce more potent and reliable BCMA-targeting bsAbs with good manufacturability and potential to be developed into therapeutic antibody drugs.

In the current study, we generated a few clones of anti-human BCMA monoclonal antibodies by DNA immunization. Using the antibody sequence from one of the clones obtained, we designed and produced a T cell-redirecting BCMA-targeting bsAb based on a FabscFv format in CHO cells. We found that the BCMA × CD3 bsAb has a good yield with minimal aggregation. We also demonstrated that our bsAb could robustly stimulate T cell proliferation and activation and efficiently induce T cell-mediated killing of MM cells both *in vitro* and *in vivo*. Thus, the results suggest that our BCMA bsAb has a good potential to be developed into a therapeutic drug for MM treatment.

MATERIALS AND METHODS

Cell lines and plasmids

Human embryonic kidney (HEK) 293 T cells, human T lymphocyte Jurkat cells and human MM cell lines RPMI8226, U266, KMS28, MM-1R and KMS11 were purchased from American Type Culture Collection (ATCC, USA). All the cell lines were cultured in RPMI 1640 (Gibco, USA) supplemented with 100 U/mL penicillin (Gibco, USA), 100 μg/mL streptomycin (Gibco, USA) and 10% fetal bovine serum (FBS) (Hyclone, USA) as described previously [18]. Full-length cDNAs encoding mouse Flt3L, GM-CSF and IL-21 and human BCMA (hBCMA) were synthesized and cloned into a pCAGGS vector. The hBCMA cDNA was also cloned into a lentiviral transfer vector pBobi, and the viral particles were packaged in HEK 293T cells with co-transfection of pMDL, pRev and pVSVG plasmids. The 293 T cells were then transduced with the lentivirus harboring the full-length cDNA encoding hBCMA and green fluorescence protein (GFP). The hBCMA-expressing 293 T cells were sorted based on GFP expression on a BD Aria cell sorter (BD Biosciences, USA).

DNA immunization hybridoma development

Balb/c mice (InVivos Pte Ltd, Singapore) were immunized with DNA plasmid in lactated Ringer's solution via hydrodynamic tail vein (HTV) injection. The mice were first primed with an injection of 10 μg mFlt3L plasmid DNA. Three days post-priming, the mice were immunized weekly with 50 μg hBCMA plus 2.5 μg mGM-CSF and 2.5 μg mIL-21 DNA plasmid via HTV injection for 4 weeks. After resting for 2 months, the mice were boosted with the last dose of HTV immunization 3 days before they were sacrificed. Splenocytes were harvested from the immunized mice and fused with SP2/0 mouse myeloma cells (ATCC, USA) using a ClonaCell™-HY Hybridoma Kit (Stem Cell Technologies, Canada). Anti-hBCMA antibody-producing clones were screened by flow cytometry using hBCMA-expressing 293 T cells.

Antibody production and purification

After subcloning the positive hybridoma clones of anti-hBCMA antibodies, the genes encoding the variable (V) region of the immunoglobulin (Ig) heavy and light chains (HC and LC) were amplified by PCR as described previously [19] and sequenced. The VH and VL gene fragments were further cloned into a tricistronic vector expressing the constant regions of trastuzumab IgG1 and a zeocin resistant gene [20] to produce the chimeric anti-hBCMA monoclonal antibodies. The expression vector for BCMA × CD3 bsAb was designed using a FabscFv-KiH format, which contains three chains—anti-BCMA LC, anti-BCMA HC with its CH3 domain engineered to form a knob and

anti-CD3 scFv linked to the engineered Fc with the CH3 domain engineered to form a hole. The design of the knob and hole in the CH3 domains was based on a previous study [21]. The expression vector of the BCMA × CD3 bsAb was constructed by inserting the synthesized internal ribosome entry site (IRES)-anti-CD3 scFv-Fc fragment downstream of the anti-BCMA HC in the tricistronic vector expressing chimeric anti-BCMA monoclonal antibody to become a tetracistronic vector. The DNA of the IRES-scFv-Fc fragment was synthesized by GenScript, USA. The constructed tricistronic or tetracistronic vectors were transfected into CHO K1 cells and selected in a medium containing zeocin to generate stably transfected pools. The anti-BCMA chimeric monoclonal antibody and BCMA × CD3 bsAb were then produced in fed-batch cultures as described previously [20].

The BCMA × CD3 bsAb was purified as previously described with minor modification [22]. Briefly, bsAb-containing supernatants were first filtered with 0.22 μm membrane to remove cell debris. The filtered supernatant was then loaded to a 5 mL HiTrap Protein A HP affinity column (GE Healthcare, USA) column at 3 mL/min using an ÄKTApurifier 100 plus (Cytiva, USA). The columns were washed using 25 mL phosphate-buffered saline (PBS) at pH 7.4, followed by elution with 25 mL of a 20 mM citric acid buffer at pH 3.0 (all at 3 mL/min). Subsequently, the post-Protein A eluate was loaded on a 5 mL HiTrap SP HP cation exchange chromatography (CEX) column (GE Healthcare, USA) at 3 mL/min. The CEX column was washed with pH 5.5 20 mM MES, followed by increasing salt concentrations of up to 0.5 M NaCl. Finally, the bsAb elute was purified by passage over a HiLoad® 16/600 Superdex® 200 pg (GE Healthcare, USA) with PBS as the running buffer. The targeted peaks were collected based on UV absorbance at 280 nm and concentrated using centrifugal filter tubes (Amicon® Ultra 15 mL Centrifugal Filters, Millipore, USA) if required. Protein quantification and purity of the final product were analyzed using HPLC-SEC with TSKgel G3000SWXL (Tosoh Bioscience, Tokyo, Japan).

SDS-PAGE and Coomassie blue staining

Purified antibodies were separated by NuPAGE® 4–12% Bis-Tris Gel (Thermo Fisher Scientific, USA) under reducing or nonreducing conditions, followed by staining with Coomassie Brilliant Blue. Briefly, 3.0 μg of purified BCMA × CD3 bsAb was either directly loaded onto the SDS-PAGE gel (nonreducing condition) or was heated at 95 °C for 5 min (reducing condition) before loading onto the gel. The electrophoresis was run in NuPAGE™ MOPS SDS Running Buffer (Thermo Fisher Scientific) at 120 V for 60 min for the non-reduced samples and NuPAGE™ MES SDS Running Buffer (Thermo Fisher Scientific, USA) for the reduced samples. After staining and washing, the gel images were taken using ChemiDoc Imaging System (Bio-Rad Laboratories, USA).

Antigen-binding assay

The binding of CD3 and BCMA by BCMA × CD3 bsAb was assessed by flow cytometry using Jurkat T and hBCMA-expressing 293T cells, respectively. Briefly, Jurkat T cells or 293T cells were plated at 2×10^5/well in a 96-well U-bottom plate. The bsAb was diluted in FACS buffer (5% FBS/PBS) at various concentrations as indicated and incubated with the cells for 15 min. After washing, the cells were further stained with a secondary PE-conjugated Goat Anti-Human IgG, Fcγ Fragment antibody (Jackson Immunoresearch Laboratories, USA) in 1:200 dilution on ice for 30 min, followed by flow cytometric analysis. hBCMA-negative parental 293T cells and CD3-negative K562 cells were used as negative controls. Data were collected on an LSR II flow cytometer (BD Biosciences, USA) and analyzed with Flowjo™ v10.7 software (BD Biosciences, USA).

T cell purification

Human peripheral blood mononuclear cells (PBMCs) were prepared from healthy donors using Ficoll-Paque PLUS (Cytiva, USA). Briefly, the whole blood was diluted with PBS and overlaid onto Ficoll and centrifuged at 500 × *g* for 30 min. The PBMCs on the interface were then collected and washed with RPMI 1640 culture medium. Total T cells were isolated from the PBMCs using a Pan T cell isolation kit (Miltenyi Biotech, Germany) according to the manufacturer's protocol. The purity of the purified T cells ($CD3^+CD56^-$) was higher than 95%, as determined by flow cytometric analysis. The use of PBMCs from healthy donors was approved Singheath Centralized Institutional Review Board (CIRB).

In vitro T cell proliferation and activation

For measuring T cell proliferation, purified T cells were first labeled with Cell Trace Violet dye (BD Biosciences, USA) in the dark for 15 min. After washing with PBS, the labeled T cells were cocultured with KMS11 cells at an effector (E): target (T) cell ratio of 1:1 in the presence of the BCMA × CD3 bsAb at the indicated concentrations for 16 h at 37 °C, supplemented with 5% CO_2 in a humidified incubator. The cells were harvested and stained with fluorescein-conjugated anti-human CD4 (BD Biosciences; SK3) and CD8 (BD Biosciences; SK1) antibodies for 30 minutes on ice in the dark, followed by flow cytometric analysis on a BD LSR II. The upregulation of CD25 and CD69 was assessed by flow cytometry. Dead cells were excluded by DAPI staining. (BD Biosciences; SK3), CD8 (BD Biosciences; SK1), CD25 (BD Biosciences; M-A251) and CD69 (BD Biosciences; FN50) antibodies for 30 min on ice in the dark. The upregulation of CD25 and CD69 was assessed by flow cytometry. Dead cells were excluded by DAPI staining.

In vitro MM cell killing assay

Two different approaches were used to assess T cell-mediated MM cell killing. For the MM cell lines without luciferase transgene, we first labeled the MM cells with Cell Trace Violet dye in the dark for 15 min. After washing with PBS, the labeled MM cells and purified T cells were seeded in 96 well in duplicates at the E:T ratio of 1:1 in RPMI cell culture medium containing 10% FBS in the presence of

the BCMA × CD3 bsAb at indicated concentrations and incubated for 48 h at 37 °C, supplemented with 5% CO_2 in a humidified incubator. The cells were harvested and stained with fluorescein-conjugated Fix Viability Dye (FVD) for 30 min at room temperature in the dark, followed by flow cytometric analysis. The viability of the MM cells was determined by the percentage of FVD-positive MM cells. For the second approach, luciferase-positive KMS11 and purified T cells were seeded in 96 well in duplicates for 48 h as described above. The viability of the KMS11 cells was assessed using Bright Glow Assay System (Promega, USA) according to the manufacturer's instructions. The percentage of MM cell killing by T cells was calculated based on the difference in the loss of luminescence of the experimental well relative to the control well containing only purified T cells with the target cells.

$$\left(\%\ \text{of killing} = \frac{\text{difference in luminescence of experimental well relative to control well}}{\text{luminescence of control well}} \times 100\right)$$

Cytokine measurement by ELISA

KMS11 and purified T cells were cultured at E:T ratio of 1:1 in the presence of BCMA × CD3 bsAb at the indicated concentrations. The culture supernatants were collected after 48 h. The T cell-secreted cytokines IFN-γ, IL-2, GM-CSF and TNFα were measured by the enzyme-linked immunosorbent assay (ELISA) using human cytokine detection kits purchased from Biolegend, USA following the manufacturer's protocol.

Establishment of mouse MM xenograft model and treatment of mice with bsAb

Eight- to ten-week-old female NSG mice (strain NOD.Cg-*Prkdc*^{scid} *Il2rg*^{tm1Wjl}/SzJ, purchased from InVivos Pte Ltd, Singapore) were given 2 × 10^6 KMS11-Luc cells via tail vein injection (i.v). Two weeks later, the mice were randomly divided into control and treatment groups based on bioluminescence intensity. Mice from the treatment group were given BCMA × CD3 bsAb i.v. (0.15 mg/kg in compound sodium lactate solution (Hartmann's Solution, B. Braun Medical Industries, Malaysia) every other day for seven doses. All animal experiments were conducted according to the guidelines approved by the Institutional Animal Care and Use Committee (IACUC) of the Agency for Science, Technology and Research.

Bioluminescence imaging

Bioluminescence of MM cells in the mice was measured with the in vivo imaging system (IVIS) (IVIS® Spectrum In Vivo Imaging System, PerkinElmer, USA). Briefly, the mice were injected i.p. with 150 mg/kg luciferin (VivoGlo™ Luciferin, Promega Corporation, USA) and anaesthetized with isoflurane. Twelve minutes post-injection, the image was taken using a charge-coupled device camera in the IVIS imaging system to evaluate the bioluminescence of MM cells in the mice. The gray-scale image of the mice was overlayed with a bioluminescence map representing the spatial distribution of photons detected from cleaved luciferin in the luciferase-expressing MM cells. Signal intensity was quantified using the Living Image Software (PerkinElmer), and the sum of all detected photon counts from the dorsal and ventral imaging was determined.

IS examination by confocal microscopy

KMS11-GFP (1 × 10^6/ml) and purified human pan-T cells (1 × 10^6/ml) were cocultured at 37 °C for 45 min in a V-well plate in the presence of BCMA × CD3 bsAb (3 μg/ml). The cells were subsequently transferred to a poly-L-lysine-coated slide and rested for 30 min to allow the cells to adhere onto the slide. The slide was next fixed with 4% paraformaldehyde in PBS for 30 min at room temperature and permeabilized with 0.1% Triton X-100 in PBS for 15 min. After washing with PBS three times each for 5 min, the cells on the slide were blocked with 5% BSA in PBST (PBS with 0.1% Tween 20) for 30 min at room temperature before being subjected to stainging with antibodies against α-actin-AF647, α-tubulin-AF647, p-Lck-AF647 or Granzyme B-AF647 together with DAPI in a humidified chamber in the dark for 1 h at room temperature or overnight at 4 °C. The slide was mounted with ProLong Diamond Antifade Mountant (Thermo Fisher, USA). The images were then acquired with an Olympus FV3000 Confocal Microscope (Olympus Corporation, Japan).

Statistical analysis

Statistical analysis was performed with GraphPad Prism 7 (GraphPad Software, USA). Two-sided independent sample Student's *t* test was used to compare the means. *P* value < 0.05 was considered significant. $^{*}P < 0.05$, $^{**}P < 0.01$ and $^{***}P < 0.001$.

RESULTS

Generation of mouse anti-human BCMA monoclonal antibodies by DNA immunization

We employed a DNA immunization followed by standard hybridoma technology to generate monoclonal antibodies (mAbs) specific for hBCMA. DNA immunization has been successfully used to develop mAbs and is amenable to the expression of membrane-bound proteins in their native forms *in vivo* [23, 24]. First, we cloned the full-length hBCMA cDNA into the pCAGGS vector, which has a synthetic CAG promoter (C: the CMV early enhancer element; A: the promoter of chicken β-actin; G: the splice acceptor of the rabbit β-globin gene), woodchuck post-transcription regulatory element (WPRE) and the rabbit β-globin polyadenylation site) and known to yield high protein expression [25, 26]. We also separately cloned several

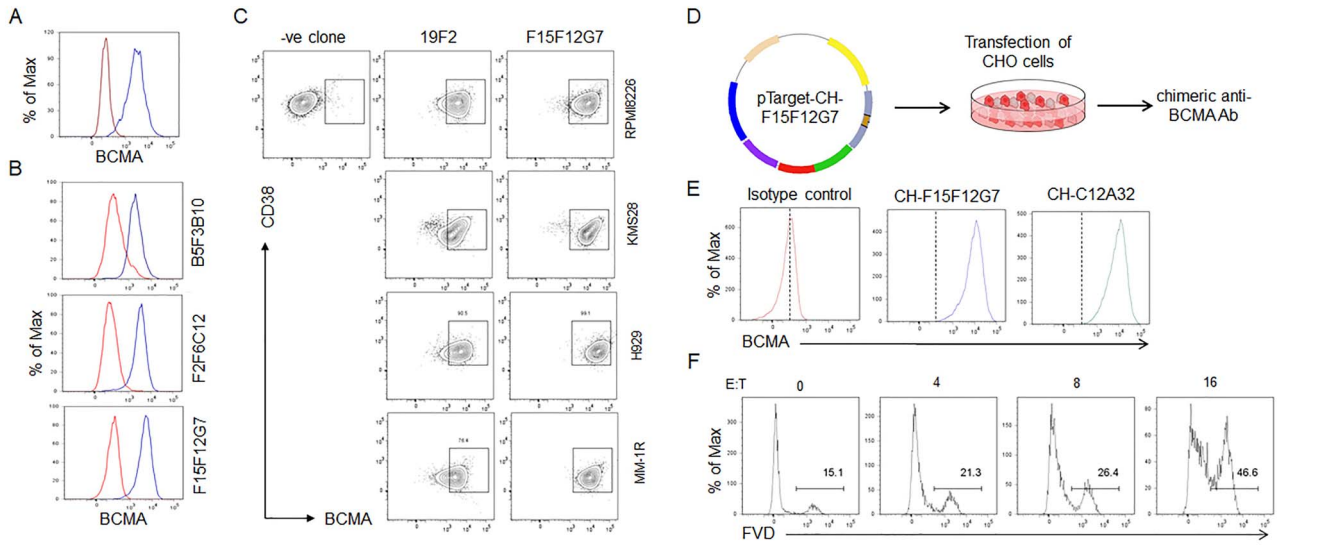

Figure 1. Generation of mouse anti-hBCMA monoclonal antibodies. (A) Detection of hBCMA on the surface of HEK 293T cells stably expressing the full-length human *BCMA*. HEK 293T cells were transduced with a lentiviral vector containing the human *BCMA* gene tagged with GFP. The GFP^+ HEK 293T cells (blue) were FACS-sorted, and the expression of BCMA on the cell surface was examined by flow cytometry using a mouse anti-human BCMA antibody. The parental HEK 293 T cells (red) were used as a negative control. (B) Validation of three clones of anti-human BCMA monoclonal antibodies by flow cytometry using hBCMA-expressing HEK 293T cells. The $hBCMA^+$ 293T cells were stained first with supernatants from subcloned three positive clones, followed by staining with a goat anti-mouse immunoglobulin Fc fragment antibody. (C) Validation of anti-hBCMA monoclonal antibody produced by clone F15F12G7 using MM cell lines RPMI 8226, KMS28, H929 and MM-1R by flow cytometry. MM cells were first stained with supernatants from clone F15F12G7, followed by staining with a goat anti-mouse immunoglobulin Fc fragment secondary antibody. Supernatants from a negative clone and a commercial mouse anti-human BCMA antibody (19F2 from Biolegend) were used as negative and positive controls, respectively. (D) Schematic diagram of production of chimeric anti-hBCMA antibodies. IgH and IgL variable region genes from the mouse monoclonal antibodies were cloned into pTarget-CH vector, which contains genes encoding for the human IgG1 heavy chain constant region gene. CHO cells were transfected with the plasmid DNA for the production of chimeric antibodies. (E) Validation of chimeric anti-hBCMA antibodies produced from CHO cell lines. The monoclonal antibodies of clone F15F12G7 produced by CHO cells were purified by protein A, and the binding to $BCMA^+$ HEK 293T cells was examined by flow cytometry. Antibody produced using a previously published sequence of anti-hBCMA monoclonal antibody C12A32 was included as the positive control, and the IgG1 isotype control antibody was used as a negative control. (F) Measurement of ADCC of anti-human BCMA antibody F15F12G7. MM cell line U266 labeled with Cell Trace Violet dye was cocultured with human PBMCs at different E:T ratios in the presence of antibody F15F12G7. After 24 h of culture, the cells were stained with fixed-viability dye, and the viability of U266 cells was examined by flow cytometry. The data shown are representative of more than three individual experiments for (A), (B), (C), (E) and (F).

mouse cytokines important for antibody response, including Flt3L, GM-CSF and IL-21, into the pCAGGS vector. We adopted a hydrodynamic tail vein (HTV) injection of plasmid DNA to immunize wild-type Balb/c mice [27]. The mouse cytokine plasmids were injected either alone or together with the hBCMA plasmid to boost the immune response.

We also generated an hBCMA-expressing HEK 293T cell line by lentiviral transduction and cell sorting based on the co-expressed GFP. The hBCMA expression on the cell surface of the sorted 293T cell was confirmed by flow cytometry using a commercially available mouse anti-hBCMA antibody (Fig. 1A). After four rounds of DNA immunization, we detected the level of anti-hBCMA antibodies in the sera of mice by flow cytometry using the hBCMA-expressing 293T cells (data not shown). Two mice with the highest titers of anti-hBCMA antibodies were selected for the last round of boosters with the hBCMA-expressing 293T cells. The splenocytes were harvested from the immunized mice and fused with SP2/0 mouse myeloma cells following the standard hybridoma protocol. Supernatants from the hybridoma clones were screened by flow cytometry using hBCMA-expressing 293T cells. The parental 293T cells were used for counterstaining to exclude the false positive clones. Several positive clones were obtained and subcloned by limiting dilution, including clones B5F3B10, F2F6C12 and F15F12G7, and validated by flow cytometry (Fig. 1B). To corroborate that the antibodies can recognize BCMA on the cell surface of MM cells, we further stained several BCMA-expressing human MM cell lines such as RPMI8226, KMS28, H929 and MM-1R using the supernatants followed by flow cytometric analysis. We could detect comparable levels of BCMA expression using our hybridoma supernatants and antibody 19F2 from Biolegend (Fig. 1C, only the result for clone F15F12G7 was shown).

Next, we amplified the genes encoding the variable (V) region of the immunoglobulin (Ig) heavy (H) and light (L) chains by RT-PCR. The VH and VL genes were sequenced and translated into amino acid sequences for a comparison with the protein sequences of the antibody purified from hybridoma supernatant and determined by mass spectrometry. After confirmation, we cloned the VH and VL fragments into a tricistronic vector pTarget-CH [28], which contains the Fc region of human IgG1, to express chimeric anti-hBCMA antibodies (Fig. 1D). The binding of the chimeric anti-hBCMA F15F12G7 antibody to hBCMA was validated by flow cytometry (Fig. 1E).

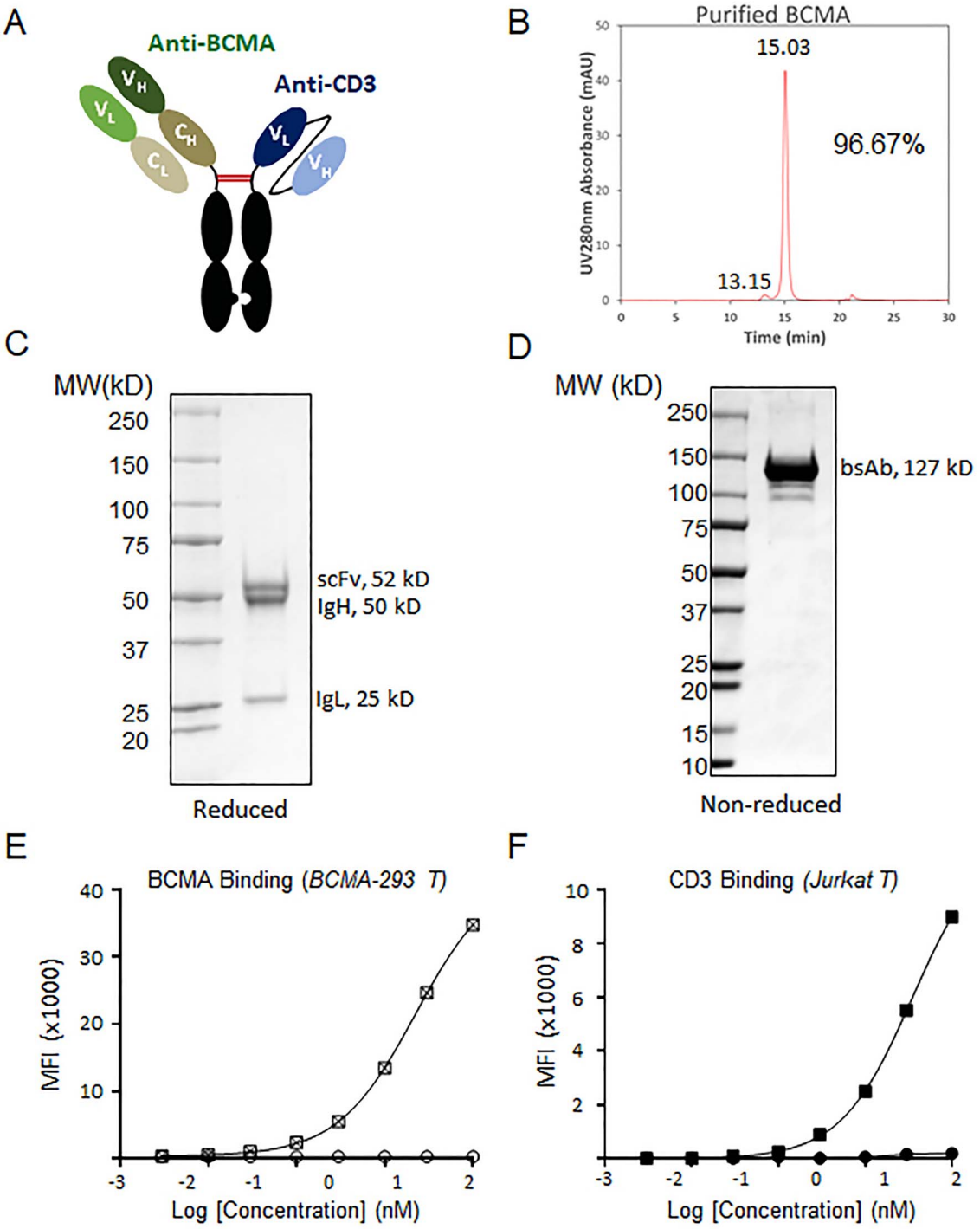

Figure 2. The design and production of BCMA × CD3 bsAb. (A) Schematic of the design of BCMA × CD3 bsAb in a FabscFv format. The BCMA × CD3 bsAb comprises a Fab arm from the anti-BCMA and an scFv arm from the anti-CD3 antibodies, respectively. The scFv arm is linked to the CH2 domain of the human IgG1 Fc fragment via the hinge region. The two arms form a heterodimeric IgG-like bsAb through the "Knob in hole" technology. The CH3 knob contains the S354C and T366W mutations, whereas the CH3 hole harbors the Y349C, T366S, L368A, and Y407V mutations, facilitating the heterodimerization. (B) Size exclusion chromatography (SEC) of the purified BCMA × CD3 bsAb produced in CHO cells. (C), (D) SDS/PAGE and Coomassie blue staining analysis of the purified BCMA × CD3 bsAb under reducing (C) and nonreducing (D) conditions. (E), (F) The binding of BCMA × CD3 bsAb to BCMA and CD3 antigens. The BCMA-expressing 293T (empty square) (E) and CD3-positive Jurkat T (filled square) (F) cells were incubated with BCMA × CD3 bsAb in various concentrations, followed by flow cytometric analysis. hBCMA-negative parental 293T (empty circle) and CD3-negative K562 cells (filled circle) were included as negative controls. The data shown are representative of more than two experiments for (C), (D), (E) and (F).

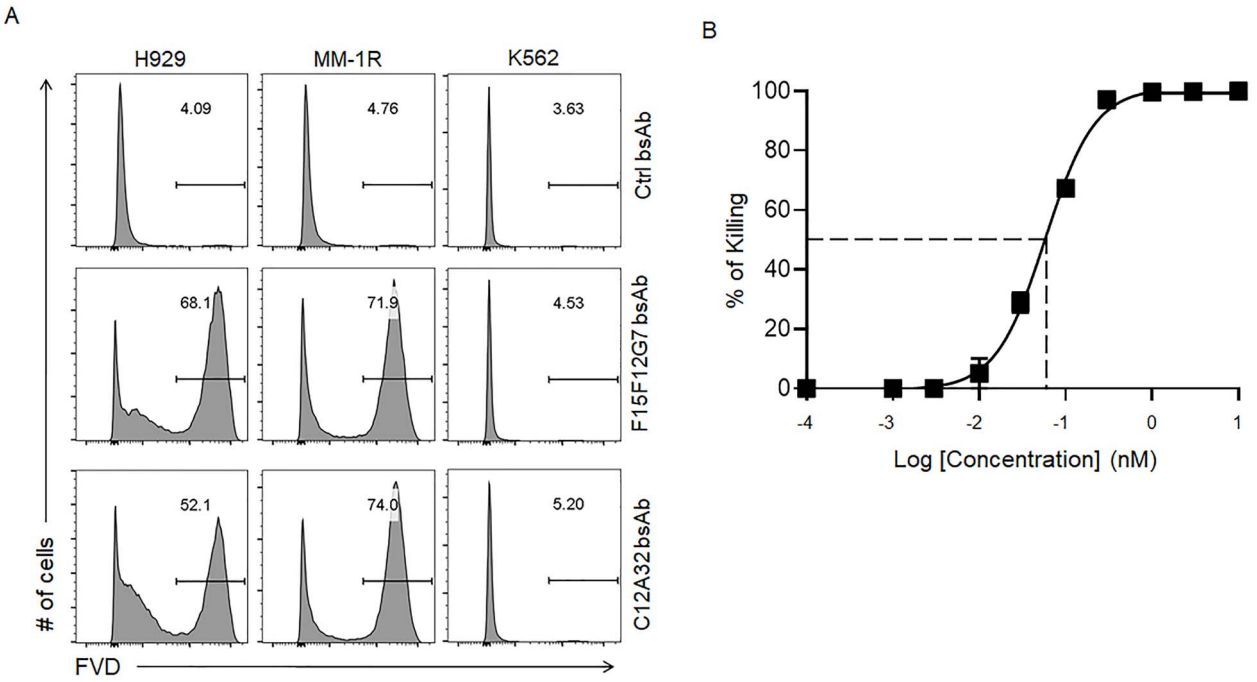

Figure 3. BCMA × CD3 FabscFv bsAb induces efficient T cell-mediated MM cell killing. (A) Flow cytometric analysis of T cell-mediated MM cell killing in the presence of BCMA × CD3 bsAb. MM cells H929 and MM-1R were labeled with Cell Trace Violet dye and cocultured with purified human T cells at 1:1 ratio for 24 h in the presence of control and BCMA × CD3 bsAb (1 nM). The MM cells were stained with FVD, and their viabilities were determined by flow cytometry. (B) The antibody dose-dependent T cell-mediated killing of MM cells by BCMA × CD3 bispecific antibody. The luciferase-positive MM cells KMS11 were cocultured with T cells at 1:1 ratio in the presence of BCMA × CD3 bsAb at the various concentrations for 48 h. The viability of KMS11 cells was measured by luminescence. The percentage of MM cell killing was calculated by the following formula: % of killing = $(OD_{\text{T cell alone}}—OD_{\text{T cell with BsAb}})/OD_{\text{T cell alone}}$. The data shown are representative of more than three (A) and 5 (B) individual experiments.

Another chimeric anti-hBCMA antibody similarly produced using the patented anti-BCMA antibody sequence (C12A32) served as a positive control. The functionality of the chimeric antibody of F15F12G7 was further assessed by measuring its antibody-dependent cellular cytotoxicity against MM cells. We found that the antibody F15F12G7 can induce efficient killing of BCMA-expressing MM cell U266 by human PBMCs at various effector (E) to target (T) cell ratios, as examined by staining MM cells with the fixed viability dye (FVD) (Fig. 1F).

Design and generation of T cell-redirecting bispecific antibody

To produce T cell-redirecting BCMA × CD3 bsAb, we designed an expression vector in a FabscFv-knob-in-hole (KiH) format. It contains three chains, anti-BCMA LC, anti-BCMA HC with its CH3 domain engineered to form a knob, and anti-CD3 scFv linked to the IgG1 Fc with the CH3 domain engineered to form a hole. The anti-BCMA HC and anti-CD3 scFv-Fc formed a heterodimer through the knob-into-hole strategy (Fig. 2A). The expression vector was transfected into CHO K1 cells to generate two stably transfected pools after selection with zeocin. Subsequently, the recovered cells were grown under fed-batch conditions. After fourteen days, the culture supernatant was harvested and subjected to titer quantification. It was noted that the two stable pools gave rise to antibody titers at 753 and 795 mg/L, respectively.

Then, we purified the BCMA × CD3 bsAb using Protein A column on an AKTA purifier 100 plus purification system, followed by cation exchange (CEX) chromatography and size-exclusion chromatography (SEC). The targeted peaks were collected based on UV absorbance at 280 nm and concentrated using Amicon Ultra centrifugal filter units if required. The purity of the bsAb was >95% as determined by HPLC-SEC (Fig. 2B). The purified bsAb was further subjected to SDS/PAGE under either reducing or nonreducing conditions, followed by Coomassie blue staining to determine bsAb integrity. The reducing SDS/-PAGE revealed the expected ~52 kDa (scFv), 50 kDa (IgH) and ~25 kDa (IgL) bands, respectively. Whereas a band about ~127 kDa in size corresponding to the full bsAb was predominantly present under the nonreducing condition (Fig. 2D).

Next, we examined the dual binding specificity of BCMA × CD3 bsAb by flow cytometric assay using the hBCMA-expressing 293 T cells and CD3-expressing human T cell line Jurkat T. We detected the specific binding of the bsAb to BCMA-expressing 293 T cells (Fig. 2E) and Jurkat cells (Fig. 2F), whereas it did not bind to BCAM-negative wild-type 293 T cells and CD3-negative K562 cells. These results suggest that the BCMA × CD3 bsAb retained the integrity and specificity of the parental anti-BCMA and anti-CD3 mAbs.

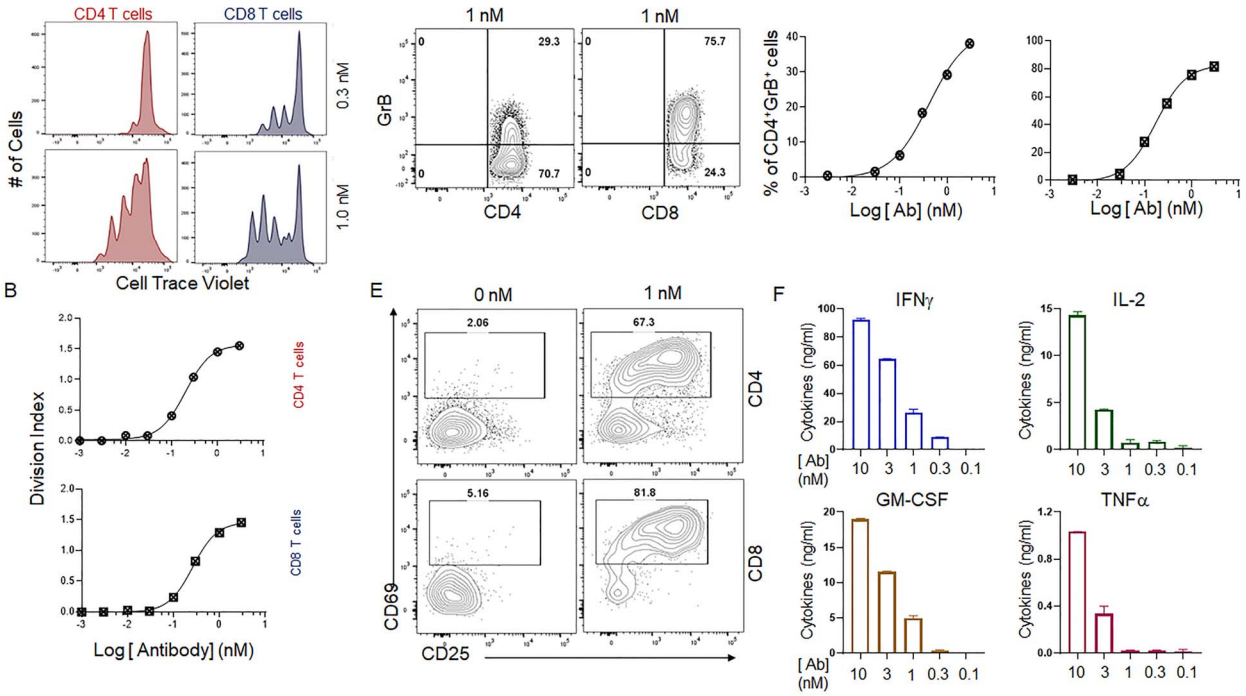

Figure 4. BCMA × CD3 FabscFv bsAb stimulates robust T cell proliferation and activation (A), (B) Flow cytometric analysis of T cell proliferation. Purified T cells were labeled with Cell Trace Violet dye and cocultured with KMS11 cells at a 1:1 ratio in the presence of 0.3 and 1 nM of BCMA × CD3 bsAb for 72 h followed by flow cytometric analysis (A). The division index of $CD4^+$ and $CD8^+$ T cells was calculated with Flow Jo software. (C) Flow cytometric analysis of Granzyme B in the $CD4^+$ and $CD8^+$ T cells cocultured with KMS11 cells in the presence of 1 nM of BCMA × CD3 bsAb for 16 h. (D) Antibody dose-dependent production of Granzyme B by $CD4^+$ and $CD8^+$ T cells. (E) Flow cytometric analysis of activation markers CD25 and CD69 in the $CD4^+$ and $CD8^+$ T cells cocultured with KMS11 cells in the absence or presence of 1 nM of BCMA × CD3 bsAb for 16 h. (F) Cytokine production by T cells. Purified T cells were cocultured with KMS11 cells in the presence of various concentrations of BCMA × CD3 bsAb. The supernatants were collected after 48 h and the production of IFNγ, IL-2, GM-CSF and TNFα were measured by ELISA. Shown are mean ± SD values for independent triplicates. The data shown are representative of more than three individual experiments.

BCMA × CD3 bsAb induces potent T cell-mediated killing of MM cells *in vitro*

Subsequently, we examined the functionality of the BCMA × CD3 bsAb by evaluating its capability of mediating T cell-directed MM cell killing *in vitro*. We first performed a flow cytometry-based *in vitro* assay by testing the bsAb's killing capability towards two BCMA-expressing MM cell lines, H929 and MM-1R. Total T cells purified from PBMCs were cocultured with the labeled MM cells at 1:1 E/T ratio in the presence of BCMA × CD3 bsAb (1 nM), and the viability of MM cells was assessed by flow cytometric assay after 48 h. Our F15F12G7 BCMA × CD3 bsAb could efficiently kill MM cells on par with another BCMA × CD3 bsAb produced in the same format using the patented C12A32 mAb sequence (Fig. 3A). A Her2 x CD3 bsAb in the same format was included as a negative control, and it did not kill MM cells due to its inability to bind to BCMA on MM cells. On the other hand, the BCMA × CD3 bsAb could not kill the BCMA-negative K562 cells, suggesting that the killing of MM cells by the bsAb is in a BCMA-specific manner.

We also performed another killing assay using the luciferase-positive KMS11-Luc MM cells, which allows us to quantify the bsAb' killing efficacy by measuring the luminescence. To this end, KMS11 and purified T cells were seeded onto the 96-well plate at 1:1 E/T ratio in duplicates in the presence of serially diluted bsAb. After 48 h of culture, we assessed the viability of the KMS11 cells by measuring the luminescence in the culture. We found that our BCMA × CD3 bsAb efficiently killed KMS11 cells, with the EC_{50} around 0.03 nM (Fig. 3B). These results suggest that our BCMA × CD3 bsAb in the FabscFv format efficiently induces T cell-mediated killing of MM cells *in vitro*.

BCMA × CD3 bsAb robustly stimulates T cell proliferation and activation *in vitro*

We further evaluated the functionality of the BCMA × CD3 bsAb in detail by assessing its ability to stimulate T cell proliferation and activation.

First, we labeled the purified T cells with Cell Trace Violet dye and cocultured them with KMS11 cells in the presence of serially diluted bsAb for four days. It was revealed that the bsAb could trigger robust $CD4^+$ and $CD8^+$ T cell proliferation as measured by the diluted cell trace violet dye signals at the antibody concentrations of 0.3 and 1.0 nM (Fig. 4A). By calculating the division index using the Flow Jo software, we were able to detect an antibody concentration-dependent proliferation of $CD4^+$ and $CD8^+$ T cells (Fig. 4B), suggesting that the BCMA × CD3 bsAb can robustly stimulate T cell proliferation *in vitro*.

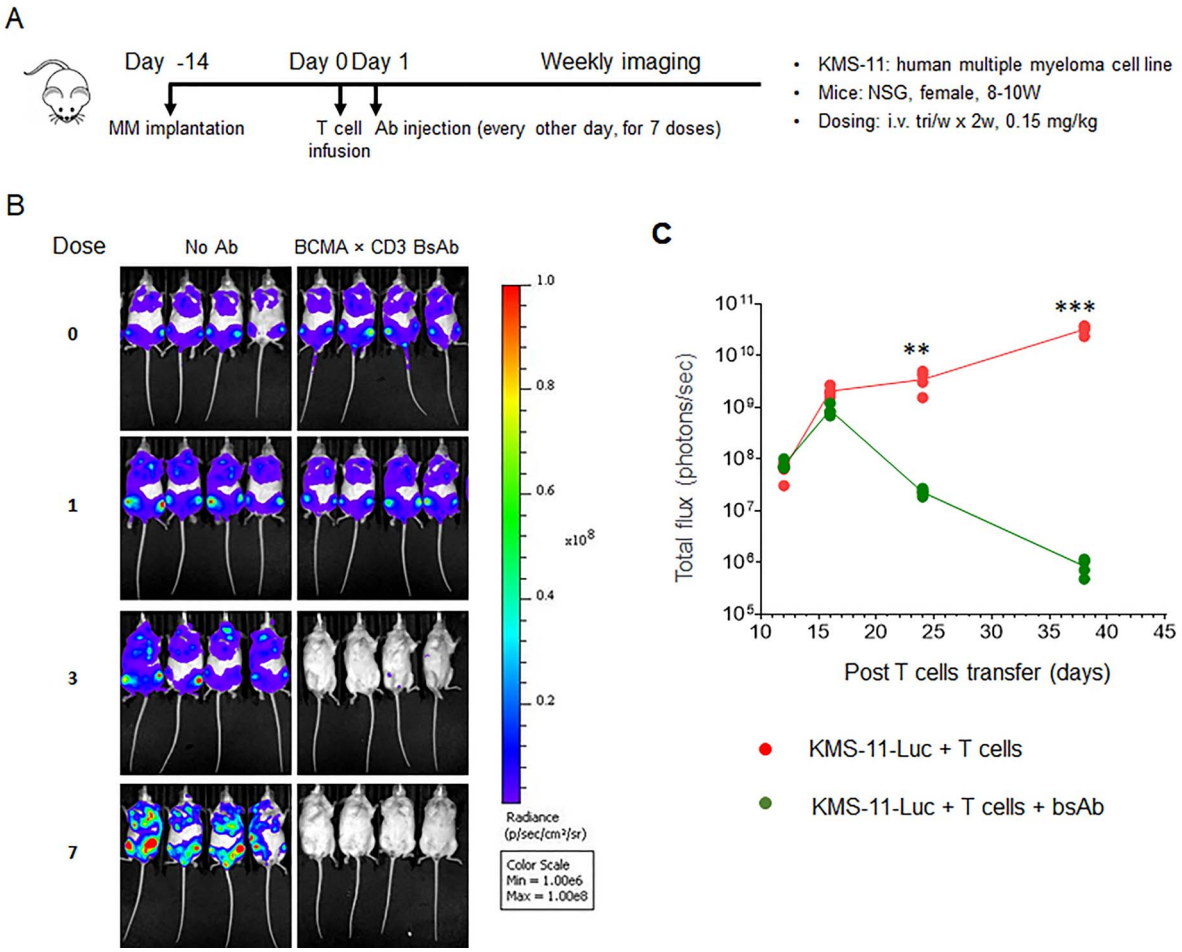

Figure 5. BCMA × CD3 BsAb efficaciously inhibits MM cell growth in NSG mice. (A) Schematic diagram of *in vivo* study BCMA × CD3 bsAb using NSG mice. 2×10^6 KMS11-Luc cells were inoculated into female NSG mice by tail vein injection (i.v) at day −14. On day 0, the mice were randomized into two groups based on the bioluminescence readings and received an infusion of 2×10^6 purified human T cells harvested from healthy donors. From day 3 onwards, one group of mice received seven doses of BCMA × CD3 bsAb (0.15 mg/kg, in sodium lactate) every other day. The control group of mice were only given the same volume of sodium lactate. Bioluminescence was measured with the IVIS Imaging System on day 0 and every 6–7 days after T cell administration to assess MM cell growth in the mice. Radiance was measured on the entire body of mice. The same longitudinal radiance color scale was applied for all IVIS imaging experiments performed on different days. (B) Sequential bioluminescence imaging of NSG mice inoculated with KMS11-Luc MM cells before bsAb treatment and after one, three and seven doses of antibody injection. (C) The *in vivo* MM growth curve of NSG mice with (green) and without (red) BCMA × CD3 bispecific antibody treatment. The radiance of bioluminescence was recorded as total flux (photons/s, mean ± SD). Statistic differences between the two groups were calculated using a two-tailed and heteroscedastic *t*-test (** $P < 0.01$ and *** $P < 0.001$). The data shown are representative of three different experiments.

We further examined the production of Granzyme B (GrB), which can activate caspases and induce target cell apoptosis, by the T cells stimulated with the BCMA × CD3 bsAb. After 16 h of coculture with KMS11 cells, the T cells were harvested and subjected to intracellular staining for GrB followed by flow cytometry. It was evident that a significant fraction of $CD4^+$ and $CD8^+$ T cells produced GrB in an antibody concentration-dependent manner (Fig. 4C and D). Similarly, the $CD4^+$ and $CD8^+$ T cells prominently upregulated the expression levels of the activation markers CD25 and CD69 upon bsAb treatment (Fig. 4E). Furthermore, we found that both $CD4^+$ and $CD8^+$ T cells produced significant levels of cytokines, including IFNγ, IL-2, GM-CSF and TNFα, in an antibody concentration-dependent manner (Fig. 4F). Thus, these results suggest that the BCMA × CD3 bsAb efficiently stimulates T cell activation and cytokine production *in vitro*.

BCMA × CD3 bsAb efficaciously inhibits MM cell growth *in vivo*

Next, we asked whether the BCMA × CD3 bsAb could suppress MM cell growth *in vivo*. To this end, we established a mouse xenograft model for human MM by inoculating KMS11-Luc cells into immune-compromised *NOD-Scid-IL2Rγ^{null}* (NSG) mice. As illustrated, the NSG mice were first engrafted with 2.0×10^6 KMS11-Luc cells by tail vein injection, followed by injection of T cells and bsAb (Fig. 5A). The *in vivo* MM cell growth was monitored by measuring the bioluminescence of MM cells in the mice weekly with the *in vivo* imaging system (IVIS). We noticed

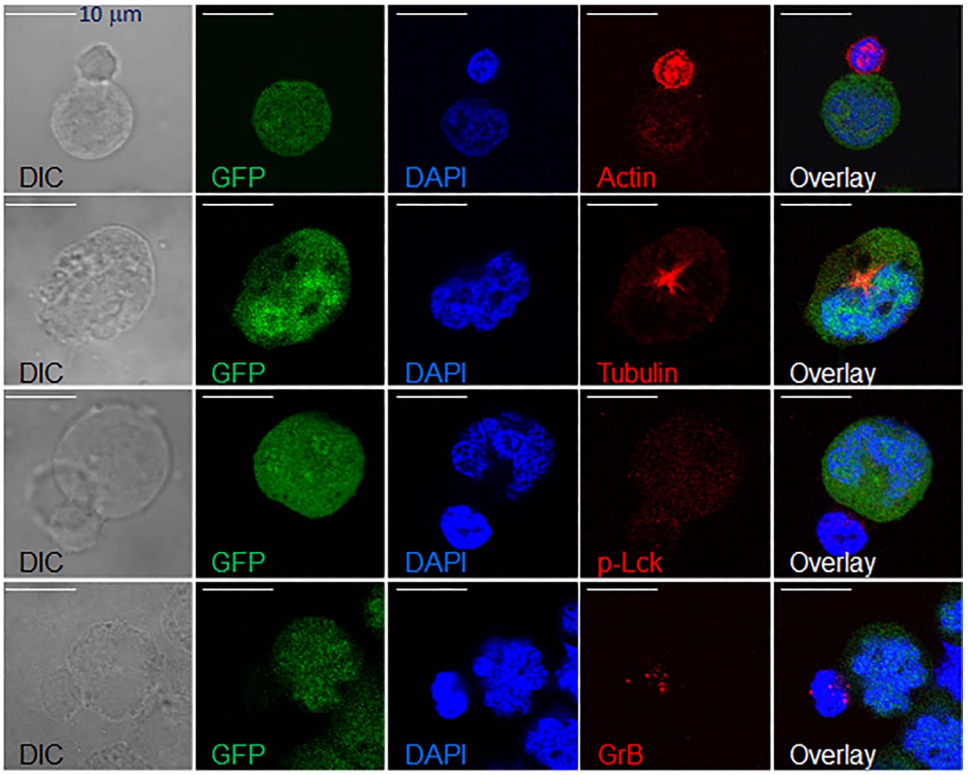

Figure 6. Formation of functional immunological synapses mediated by BCMA × CD3 bsAb. GFP$^+$ KMS11 and purified human T cells were cocultured in the presence of BCMA × CD3 bsAb (3 μg/ml) at 37 °C for 45 min on a poly-L-lysine-coated. After fixation, permeabilization and staining, the slide was examined by confocal microscopy to detect α-actin, α-tubulin, p-Lck, and Granzyme B. KMS11 cells were detected as GFP-positive cells. All nuclei were counterstained with 4′,6-diamidino-2-phenylindole (DAPI). Fluorochromes used are α-actin (AF647), α-tubulin (AF647), p-Lck (AF647), and Granzyme B (AF647). DIC, differential interference contrast.

that the KMS11-Luc grew quite fast, with the bioluminescence intensity going up to 10^8 photons/s. Interestingly, the mice receiving T cells and three doses of bsAb injection had significantly reduced *in vivo* MM growth compared to those injected with T cells alone, as evidenced by luminescence images (Fig. 5B). By quantifying the luminescence intensity of the mice, we found that the luminescence intensity was about 100 folds in the mice treated with the bsAb compared to the mice in the T cell alone group (Fig. 5C). After 7 doses of injection, the difference was even more drastic, with MM cells growing vigorously in the mice of the T cell alone group, while the mice in the bsAb-treatment group had even more reduced tumor burden (Fig. 5B and C). These results suggest the bsAb can efficiently suppress MM cell growth *in vivo* through engaging T cells.

BCMA × CD3 bsAb mediates the formation of the functional immunological synapse

Next, we attempted to understand the molecular mechanism whereby the BCMA × CD3 bsAb mediates the robust T cell-mediated killing of MM cells. Under physiological conditions, a stable cell–cell junction between T cells and antigen-presenting cells (APCs) T cells, also called the immunological synapse (IS), is formed at the interface of T cells interaction with APCs. IS is known to be essential for T cell activation and acquisition of effector functions [29]. Recent studies also demonstrated that tumor-associated antigen-targeting bsAb mediated IS assembly between tumor and T cells [30, 31]. Thus, we asked if the BCMA × CD3 bsAb can induce the formation of functional IS between T and MM cells. To this end, we first examined the microtubule-organizing center (MTOC) polarization and filamentous actin (F-actin) accumulation in the culture with bsAb by confocal microscopy. After coculture of KMS11 and T cells in the presence of bsAb, we could detect an accumulation of α-actin and α-tubulin (red), which is indicative of a functional IS, at the interface between the GFP$^+$ KMS11 (green) and T (blue, as stained with DAPI) (Fig. 6, first two rows). Moreover, we could also detect the accumulation of Granzyme B and phosphorylated Lck (red) at the boundary between KMS11 and T cells (Fig. 6, last two rows). Together, these data indicate that BCMA × CD3 bsAb induces functional IS formation between MM and T cells to mediate T cell activation and MM cell killing by T cells.

DISCUSSION

This study reports the design and production of a T cell-redirecting BCMA-targeting BCMA × CD3 bsAb. The bsAb is designed in a "1 + 1" FabscFv format with a Fab arm binding hBCMA on MM cells and the scFv

arm recognizing CD3 on T cells. We show that the bsAb can robustly stimulate T cell proliferation, upregulation of activation markers and production of granzyme B and various cytokines upon coculture with BCMA-expressing MM cells. Furthermore, we demonstrate that the bsAb can efficiently induce MM cell killing *in vitro* and potently suppress MM cell growth *in vivo* mediated by T cells.

We previously tested multiple formats for developing T cell-redirecting bsAb using anti-Her2 antibody as the antibody against the tumor-associated antigen (TAA). Among the formats examined, the FabscFv format was found to give the best bsAb yield and the least mismatch and aggregation of antibody fragments (manuscript under review). In this study, we design the BCMA × CD3 FabscFv bsAb based on our poly-cistronic vector described previously [28]. The gene fragments encoding anti-BCMA IgL, anti-BCMA IgH and anti-CD3 scFv are all cloned into a single polycistronic expression vector, warranting a well-controlled and comparable expression level for individual antibody domain fragments and a significantly simplified process for developing the bsAb-producing CHO cell line. Our optimized polycistronic vector yielded a decent antibody titer at close to 0.8 g/L, which is desirable for the production of bsAb. Moreover, the Fc KiH technology was used in our design to avoid the formation of homodimers.

We also streamlined a purification strategy for the bsAb based on a previously optimized downstream purification process [32]. The IgG-like bsAb in the culture supernatant was first enriched with the Protein A affinity chromatography. The mispaired and/or unwanted fragments were further removed with the CEX chromatography, improving the bsAb purity significantly up to 90%. After the final polishing with the size exclusion chromatography (SEC), the purity of the bsAb is more than 96%. Though the Fc KiH technology can significantly reduce the chance of forming homodimers during the bsAb production, some studies showed that homodimer by-products were frequently found [31, 32]. In our study, the bsAb was designed in an asymmetric format, such that the homodimers are quite different from the heterodimer in terms of their molecular weight and the charge. Therefore, the homodimers can be readily removed by CEX and SEC during the purification process.

The bsAb also exhibited potent efficacy in stimulating T cell proliferation and activation, apart from the high yield and purity. The T cell-redirecting BCMAxCD3 bsAb has two arms, with one arm targeting the CD3ε chain of the TCR complex and the other arm recognizing BCMA expressed on the MM cells. Therefore, the bsAb can bridge T and MM cells together, mimicking natural TCR:pMHC engagement when T cells are activated by antigens presented by MHC molecules and triggering T-cell activation and proliferation [33]. Consequently, we found that the bsAb could efficiently kill BCMA-expressing MM cells *in vitro* and *in vivo*. Interestingly, we noticed that the bsAb could induce granzyme B expression robustly in both $CD4^+$ and $CD8^+$, indicating that both of them can kill target cells in the presence of bsAb. This finding is consistent with recent findings that CD4 cytotoxic T cells are also important for anti-tumor immunity and have potential use in immunotherapy for specific cancers [34].

Hence, our study demonstrates that the FabscFv is an acceptable format for producing BCMA × CD3 bsAb with good drug developability and promising potential to be developed into a therapeutic antibody drug for the treatment of MM.

FUNDING STATEMENT

This work was funded by Singapore Agency for Science Technology and Research.
Conflict of Interest Statement: None.

DATA AVAILABILITY

The sequences of the mAb and bsAb are proprietary and cannot be shared publicly. The rest of the data can be shared upon reasonable request to the corresponding author.

ETHICS AND CONSENT STATEMENT

The use of PBMCs from healthy donors in this study was approved by Singhealth Centralized Institutional Review Board exemption (CIRB Ref: 2017/2471).

ANIMAL RESEARCH

All animal experiments were conducted according to the guidelines approved by the Institutional Animal Care and Use Committee (IACUC) of the Agency for Science, Technology and Research.

REFERENCES

1. Dimopoulos, MA, Richardson, PG, Moreau, P *et al.* Current treatment landscape for relapsed and/or refractory multiple myeloma. *Nat Rev Clin Oncol* 2015; **12**: 42–54.
2. Cerchione, C, Usmani, SZ, Stewart, AK *et al.* Gene expression profiling in multiple myeloma: redefining the paradigm of risk-adapted treatment. *Front Oncol* 2022; **12**: 820768.
3. Lonial, S, Dimopoulos, M, Palumbo, A *et al.* Elotuzumab therapy for relapsed or refractory multiple myeloma. *N Engl J Med* 2015; **373**: 621–31.
4. Pazina, T, James, AM, MacFarlane, AWT *et al.* The anti-SLAMF7 antibody elotuzumab mediates NK cell activation through both CD16-dependent and -independent mechanisms. *Onco Targets Ther* 2017; **6**: e1339853.
5. Palumbo, A, Chanan-Khan, A, Weisel, K *et al.* Daratumumab, bortezomib, and dexamethasone for multiple myeloma. *N Engl J Med* 2016; **375**: 754–66.
6. Stewart, AK, Rajkumar, SV, Dimopoulos, MA *et al.* Carfilzomib, lenalidomide, and dexamethasone for relapsed multiple myeloma. *N Engl J Med* 2015; **372**: 142–52.
7. Moreau, P, Kumar, SK, San Miguel, J *et al.* Treatment of relapsed and refractory multiple myeloma: recommendations from the international myeloma working group. *Lancet Oncol* 2021; **22**: e105–18.
8. Sperling, AS, Anderson, KC. Facts and hopes in multiple myeloma immunotherapy. *Clin Cancer Res* 2021; **27**: 4468–77.
9. Hideshima, T, Bergsagel, PL, Kuehl, WM *et al.* Advances in biology of multiple myeloma: clinical applications. *Blood* 2004; **104**: 607–18.
10. Tai, YT, Acharya, C, An, G *et al.* APRIL and BCMA promote human multiple myeloma growth and immunosuppression in the bone marrow microenvironment. *Blood* 2016; **127**: 3225–36.
11. Day, ES, Cachero, TG, Qian, F *et al.* Selectivity of BAFF/BLyS and APRIL for binding to the TNF family receptors BAFFR/BR3 and BCMA. *Biochemistry* 2005; **44**: 1919–31.

12. Xu, S, Lam, KP. B-cell maturation protein, which binds the tumor necrosis factor family members BAFF and APRIL, is dispensable for humoral immune responses. *Mol Cell Biol* 2001; **21**: 4067–74.
13. O'Connor, BP, Raman, VS, Erickson, LD *et al.* BCMA is essential for the survival of long-lived bone marrow plasma cells. *J Exp Med* 2004; **199**: 91–8.
14. Cho, SF, Xing, L, Anderson, KC *et al.* Promising antigens for the new frontier of targeted immunotherapy in multiple myeloma. *Cancers (Basel)* 2021; **13**(24): 6136–58.
15. Xu, S, Lam, KP. Transmembrane activator and CAML interactor (TACI): another potential target for immunotherapy of multiple myeloma? *Cancers (Basel)* 2020; **12**(4): 1045–58.
16. Cho, SF, Lin, L, Xing, L *et al.* Monoclonal antibody: a new treatment strategy against multiple myeloma. *Antibodies (Basel)* 2017; **6**(4): 18–39.
17. Caraccio, C, Krishna, S, Phillips, DJ *et al.* Bispecific antibodies for multiple myeloma: a review of targets, drugs, clinical trials, and future directions. *Front Immunol* 2020; **11**: 501.
18. Huo, J, Xu, S, Lin, B *et al.* Fas apoptosis inhibitory molecule is upregulated by IGF-1 signaling and modulates Akt activation and IRF4 expression in multiple myeloma. *Leukemia* 2013; **27**: 1165–71.
19. von Boehmer, L, Liu, C, Ackerman, S *et al.* Sequencing and cloning of antigen-specific antibodies from mouse memory B cells. *Nat Protoc* 2016; **11**: 1908–23.
20. Yeo, JHM, Ho, SCL, Mariati, M *et al.* Optimized selection marker and CHO host cell combinations for generating high monoclonal antibody producing cell lines. *Biotechnol J* 2017; **12**(12): 1700175–182.
21. Merchant, AM, Zhu, Z, Yuan, JQ *et al.* An efficient route to human bispecific IgG. *Nat Biotechnol* 1998; **16**: 677–81.
22. Chen, SW, Tan, D, Yang, YS *et al.* Investigation of the effect of salt additives in protein L affinity chromatography for the purification of tandem single-chain variable fragment bispecific antibodies. *MAbs* 2020; **12**: 1718440.
23. Wolff, JA, Malone, RW, Williams, P *et al.* Direct gene transfer into mouse muscle in vivo. *Science* 1990; **247**: 1465–8.
24. Kofta, W, Wedrychowicz, H. C-DNA vaccination against parasitic infections: advantages and disadvantages. *Vet Parasitol* 2001; **100**: 3–12.
25. Ramezani, A, Hawley, TS, Hawley, RG. Lentiviral vectors for enhanced gene expression in human hematopoietic cells. *Mol Ther* 2000; **2**: 458–69.
26. Hazen, M, Bhakta, S, Vij, R *et al.* An improved and robust DNA immunization method to develop antibodies against extracellular loops of multi-transmembrane proteins. *MAbs* 2014; **6**: 95–107.
27. Chen, Q, He, F, Kwang, J *et al.* GM-CSF and IL-4 stimulate antibody responses in humanized mice by promoting T, B, and dendritic cell maturation. *J Immunol* 2012; **189**: 5223–9.
28. Ho, SC, Bardor, M, Feng, H *et al.* IRES-mediated tricistronic vectors for enhancing generation of high monoclonal antibody expressing CHO cell lines. *J Biotechnol* 2012; **157**: 130–9.
29. Fooksman, DR, Vardhana, S, Vasiliver-Shamis, G *et al.* Functional anatomy of T cell activation and synapse formation. *Annu Rev Immunol* 2010; **28**: 79–105.
30. Harwood, SL, Alvarez-Cienfuegos, A, Nunez-Prado, N *et al.* ATTACK, a novel bispecific T cell-recruiting antibody with trivalent EGFR binding and monovalent CD3 binding for cancer immunotherapy. *Onco Targets Ther* 2017; **7**: e1377874.
31. Li, J, Stagg, NJ, Johnston, J *et al.* Membrane-proximal epitope facilitates efficient T cell synapse formation by anti-FcRH5/CD3 and is a requirement for myeloma cell killing. *Cancer Cell* 2017; **31**: 383–95.
32. Chen, SW, Zhang, W. Current trends and challenges in the downstream purification of bispecific antibodies. *Antib Ther* 2021; **4**: 73–88.
33. Wu, Z, Cheung, NV. T cell engaging bispecific antibody (T-BsAb): from technology to therapeutics. *Pharmacol Ther* 2018; **182**: 161–75.
34. Oh, DY, Fong, L. Cytotoxic CD4(+) T cells in cancer: expanding the immune effector toolbox. *Immunity* 2021; **54**: 2701–11.